Coupling between detailed building energy models and a data driven urban canopy model

Martin, Miguel; Berges, Mario; Stoter, Jantien; Garcia Sanchez, Clara

Publication date
2024

Document Version
Final published version

Published in
PLEA 2024: (Re)Thinking Resilience

Proceedings of 37th PLEA Conference,
26-28 June 2024 Wrocław, Poland

PLEA 2024: (RE)THINKING RESILIENCE

The book of proceedings

Editors: Barbara Widera, Marta Rudnicka-Bogusz,
Jakub Onyszkiewicz, Agata Woźniczka

PLEA 2024: (RE)THINKING RESILIENCE

Proceedings of 37th PLEA Conference, Sustainable Architecture and Urban Design

26-28 June 2024 Wrocław, Poland
Wrocław University of Science and Technology

Editors: Barbara Widera, Marta Rudnicka-Bogusz, Jakub Onyszkiewicz, Agata Woźniczka

Organised by: PLEA, Fundacja PLEA 2024 Conference

Honorary Patronage: Rector of Wrocław University of Science and Technology,
Prof. Arkadiusz Wójs, DSc, PhD, Eng.

Scientific Patronage: The Committee for Architecture and Town Planning of the Wrocław Branch of the Polish Academy of Sciences

Wrocław University of Science and Technology Publishing House
Wybrzeże Wyspiańskiego 27, 50-370 Wrocław
http://www.oficyna.pwr.edu.pl
e-mail: oficwyd@pwr.edu.pl
zamawianie.ksiazek@pwr.edu.pl

ISBN 978-83-7493-275-2
https://doi.org/10.37190/PLEA_2024

Coupling between detailed building energy models and a data driven urban canopy model

MIGUEL MARTIN,[1] MARIO BERGES,[2] JANTIEN STOTER,[1]
CLARA GARCIA SANCHEZ,[1]
[1] Delft University of Technology, Delft, The Netherlands
[2] Carnegie Mellon University, Pittsburgh, United States

ABSTRACT: This paper describes a data driven urban canopy model that can be coupled with detailed building energy models. The data driven model is used to assess the outdoor air temperature and humidity in a street canyon considering as inputs weather conditions at the atmospheric layer, the surface temperature of surrounding building facades and the street, and the heat released from the use of air-conditioning. Predictions made by the model were tested using measurements of the outdoor air temperature and humidity collected between April and August 2019 in Singapore. Results show that the model estimates the outdoor air temperature with a similar accuracy than others that were validated using the same input and test data, while providing estimates with a higher temporal resolution and considering urban morphology with a higher fidelity. They also demonstrate that the model can predict the impact of waste heat releases and cool pavement on the outdoor air temperature and building energy consumption. In the future, vegetation could be considered as an input of the model if the land surface temperature is measured using an infrared thermal camera. Another improvement would be to define weather conditions at the atmospheric layer from rooftop measurements or a climate model.
KEYWORDS: Urban heat island, Urban canopy modelling, Building energy modelling, Machine learning, Mitigation strategies

1. INTRODUCTION

For the last three centuries, most cities in the world have considerably expanded to accommodate their inhabitants. By 2050, it is expected that almost two thirds of the world's population will live in urban areas [1]. This trend in urbanization is the cause of several climatic hazards, including Urban Heat Islands (UHIs). UHIs primarily result from the heat accumulated in cities and the wind breeze obstructed by buildings. They provoke serious thermal discomfort in the outdoor environment and increases in the energy consumed in indoor spaces. The former consequence of UHIs has been declared a major threat to public health since the heat wave episodes of the summer 2023 in various parts of the world [2].

Given the influence of urbanization on UHIs, urban planning plays a major role to improve outdoor thermal comfort and minimize building energy consumption [3, 4]. To determine benefits of mitigations strategies to UHIs before their implementation, urban planners can now count on virtual replicates or digital twins of a city. City Digital Twins (CDTs) essentially consist of 3D city models to display the geometry of buildings, sensor data to monitor the indoor and outdoor built environment, and models to predict or prevent undesirable events that might occur in the city [5-7]. Whatever model is integrated into a CDT, it must meet certain requirements. One of them is to consider the urban morphology with the Level of Detail (LoD) expressed in the 3D city model [8]. Another one is that simulations using the model can be performed with low computational efforts. The latter requirement is particularly relevant for urban planners to make quick decisions on the strategies to adopt for mitigating UHIs.

To study UHIs through a CDT, it is necessary to include models that can perform simulations of interactions between buildings and their outdoor environment at the neighbourhood or city scale. The reason is the heat transferred from the envelope of buildings to the outdoor air is an important factor of UHIs [9]. In return, the outdoor air temperature and humidity strongly affect the energy consumed by buildings to maintain an appropriate level of thermal comfort [10]. Every increase in the energy consumed by buildings for cooling their respective indoor space is translated into an augmentation of waste heat releases, another important factor of UHIs.

Interactions between buildings and their outdoor environment are simulated using two coupled models: the Building Energy Model (BEM) and the Urban Microclimate Model (UMM) [11]. The former component assesses the energy consumed by a building, while the latter estimates outdoor conditions at the urban microscale, that is within a range of less than one kilometre. When the two components are coupled, the outputs obtained from one are iteratively used to define boundary conditions of the other until the end of simulations.

A first category of UMM, known as physically-based Urban Canopy Models (UCMs), predicts outdoor temperature and humidity within a street canyon using a sensible and latent heat balance, respectively [12]. The heat balances describe time variations of the outdoor air temperature and humidity within the street canyon with respect to heat fluxes coming from surrounding surfaces and anthropogenic heat sources. The street canyon is either considered as a single air volume or a stack of multiple air volumes. In either case, physically-based UCMs assume that buildings are cubes with similar dimensions which are separated by streets of equal widths. It means they consider the urban morphology with a low level of detail, which is a major limitation to integrate them in a CDT.

To estimate outdoor conditions at the neighbourhood scale, while considering the urban morphology with a higher level of detail, studies have used computational fluid dynamics to approximate the wind flow and outdoor air temperature within a neighbourhood [13]. In addition to performing simulations using complex urban morphologies, this physically-based method provides estimates of outdoor conditions with a high spatial resolution. The temporal resolution, however, remains limited due to tremendous computational efforts that are required to perform simulations.

A recent review published by Wang et al. [14] demonstrates that the outdoor air temperature in the urban canopy layer can be assessed with a high temporal resolution using Data Driven Models (DDMs). These DDMs take as inputs land surface measurements collected by remote sensing and atmospheric weather conditions obtained by simulations. Both remote sensed data and weather simulated data are given at the mesoscale. In the majority of studies, these input data, together with measurements of the outdoor air temperature, are used to train and test two kinds of regression models, namely tree based models or artificial neural networks. The former type of DDMs usually fail in predicting the extreme values for the outdoor air temperature, while the latter model requires a large dataset and high computational efforts to be trained and tested. Whether a tree based model or artificial neural network is used as a DDM, it does not take into account how the outdoor air temperature at a specific point is affected by surrounding physical entities at the urban microscale, in particular buildings.

To consider buildings while predicting the outdoor air temperature at a specific location with a high temporal resolution, this paper describes a DDM that can be coupled with detailed BEMs. As most models shown in the literature, the DDM also considers as inputs atmospheric weather conditions and the land surface temperature. However, the land surface temperature is assumed to be obtained from a contact surface sensor or a thermal camera, which enable capturing the microscale effect of the street surface more accurately than a satellite.

Using the coupling between detailed BEMs and the DDM, the purpose of this study is to show that (1) outdoor air temperature and humidity in a street canyon can be predicted with a high temporal resolution and acceptable accuracy, (2) observations can be made on the impact of waste heat releases on the outdoor air temperature and the building energy use, and (3) it is possible to see how the outdoor environment and the building consumption are affected by cool pavement.

2. METHODOLOGY

2.1 The data-driven urban canopy model

The most important contribution of this work lies in a DMM that can predict outdoor air temperature and humidity in a street canyon with a high level of detail. The DDM is trained and tested using data collected by a series of weather stations in the street canyon. The weather stations should at least measure the outdoor air temperature, relative humidity, and pressure, so that the average outdoor air temperature ($\bar{T}_{can}$) and specific humidity ($\bar{q}_{can}$) at each time (t) in the street canyon can be observed and predicted.

Assuming the street canyon as a single layer, that is an air volume with uniform temperature and humidity, $\bar{T}_{can}$ and $\bar{q}_{can}$ are governed by sensible and latent heat balances, which can be expressed as:

$$V_{can} c_p \rho \frac{d\bar{T}_{can}}{dt} = \sum_{m=1}^{M} h_m A_m (\bar{T}_m - \bar{T}_{can}) + \sum_{n=1}^{N} H_n \qquad (1)$$

$$V_{can} c_p \rho \frac{d\bar{q}_{can}}{dt} = \sum_{p=1}^{P} h_p A_p (\bar{q}_p - \bar{q}_{can}) + \frac{c_p}{L} \sum_{q=1}^{Q} LE_q \qquad (2)$$

where V_{can} is the air volume of the street canyon (in m^3), c_p the specific heat capacity of dry air (in J/kg-K), ρ its density (in kg/m^3), L the latent heat of water vaporization (in J/kg), $\bar{T}_m$ the average temperature either of surrounding building facades, atmospheric layer, pavement, or vegetation (in ^{o}C), h_m or h_p their convective heat transfer coefficient (in W/m^2-K), A_m or A_p their surface area (in m^2), $\bar{q}_p$ their average specific humidity (in kg/kg), H_n the sensible heat released either from surrounding buildings or traffic (in W), E_q their rate of evaporation (in kg/s), m and p indices of thermal nodes, and n and q indices of sensible and latent heat sources. Equations (1) and (2) can be formulated as a linear state space model, such that:

$$\dot{\boldsymbol{x}} = \boldsymbol{A} \cdot \boldsymbol{x} + \boldsymbol{B} \cdot \boldsymbol{u} \qquad (3)$$

$$\boldsymbol{y} = \boldsymbol{C} \cdot \boldsymbol{x} + \boldsymbol{D} \cdot \boldsymbol{u} \qquad (4)$$

where $\boldsymbol{u} = [\bar{T}_1, \dots, \bar{T}_M, H_1, \dots, H_N, \bar{q}_1, \dots, \bar{q}_P, E_1, \dots, E_Q\,]^T$ and $\boldsymbol{x} = [\bar{T}_{can}, \bar{q}_{can}]^T$. From this formulation of sensible and latent heat balances, the DDM uses either a explicit or implicit time discretization scheme to predict state variables $\boldsymbol{x}_k$ at different time steps $t_k =$

$t_0 + k\Delta t$ as shown in Figure 1. Matrices $\boldsymbol{A_d}$, $\boldsymbol{B_d}$, $\boldsymbol{C_d}$, and $\boldsymbol{D_d}$ are derived from matrices $\boldsymbol{A}$, $\boldsymbol{B}$, $\boldsymbol{C}$, and $\boldsymbol{D}$, respectively, using a time discretization scheme.

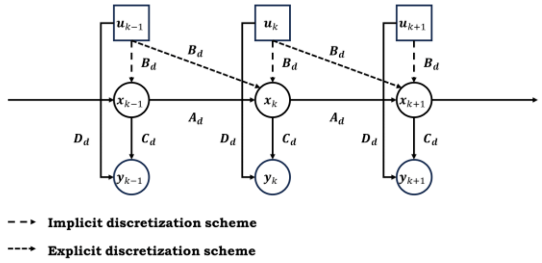

Figure 1. Discrete linear state space model used to predict outdoor air temperature and humidity in a street canyon.

Using the discrete linear state space model, the training phase of the DDM consists of finding the vector $\boldsymbol{h}$ of convective heat transfer coefficients that minimizes the discrepancy between estimates of $\overline{T}_{can}$ and $\overline{q}_{can}$ and their measurements. The training phase is thus expressed as a constrained multi-objective optimization so that:

$$\underset{\boldsymbol{h}}{\operatorname{argmin}}\, l^2\left(\overline{T}^e{}_{can} - \overline{T}^m{}_{can}\right), l^2\left(\overline{q}^e{}_{can} - \overline{q}^m{}_{can}\right) \quad (5)$$
$$h_{lb} \le h_m \le h_{up}$$

where l^2 is the root mean square error with respect to the time discretization of the linear state space model, $\overline{T}^e{}_{can}$ and $\overline{q}^e{}_{can}$ estimates of the outdoor air temperature and humidity by the discrete linear state space model, respectively, $\overline{T}^m{}_{can}$ and $\overline{q}^m{}_{can}$ their measurements by weather stations in the street canyon, and h_{lb} and h_{up} the lower and upper bounds of convective heat transfer coefficients.

2.2 Coupling with detailed building energy models

The input vector ($\boldsymbol{u}_k$) of the discrete linear state space model is iteratively evaluated at each timestep (k) from different sources of information. Firstly, $\boldsymbol{u}_k$ consists of air temperature and humidity at the atmospheric level, which can be obtained either from measurements of a rural weather station or simulated data resulting from a climate model. Secondly, it consists of information measured or estimated at the street level. The surface temperature and humidity of pavement and vegetation, for instance, is assumed to be measured by a contact surface sensor or an infrared thermal camera. On the other hand, the sensible and latent heat released by traffic is usually assessed from an empirical model as in Grimmond [15]. Lastly, $\boldsymbol{u}_k$ is primarily composed of information that is simulated by detailed building energy models. It includes the surface temperature of surrounding facades and the waste heat releases.

Outputs ($\boldsymbol{y}_k$) provided by the discrete linear state space model after training and testing phases are used to specify boundary conditions of detailed BEMs. By default, boundary conditions of detailed BEMs are defined from typical meteorological data collected from a rural weather station. These meteorological data are iteratively replaced by $\boldsymbol{y}_k$ until a convergence criteria is achieved. The convergence criteria is established using the average sensible ($\overline{H}_{sys}$) and latent ($\overline{LE}_{sys}$) load of surrounding buildings so that:

$$l^2\left(\overline{H}^{n+1}_{sys} - \overline{H}^{n}_{sys}\right) \le \varepsilon_{\overline{H}_{sys}} \text{ and}$$
$$l^2\left(\overline{LE}^{n+1}_{sys} - \overline{LE}^{n}_{sys}\right) \le \varepsilon_{\overline{LE}_{sys}} \quad (6)$$

where $\overline{H}^{n}_{sys}$ and $\overline{LE}^{n}_{sys}$ are the average sensible and latent loads estimated by detailed BEMs at the n-th iteration of the one-time-step dynamic coupling with the DDM. Figure 2 illustrates the coupled scheme between detailed BEMs and the DDM.

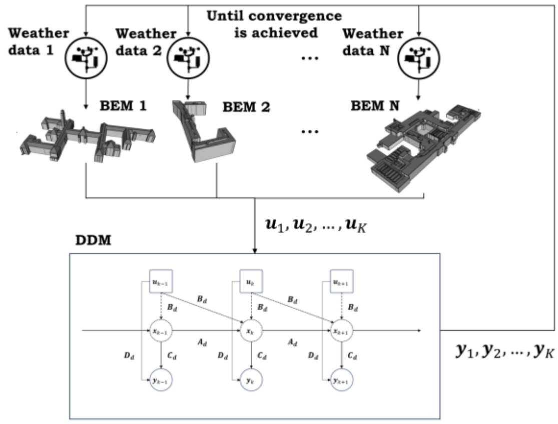

Figure 2. Coupling between detailed BEMs and the DDM.

2.3 Cool pavement

Cool pavement is a countermeasure to UHIs, whose effect on the outdoor air temperature and building energy consumption can be considered by the coupled scheme. The effect of cool pavement is assessed by modifying the surface temperature of the pavement ($\overline{T}_{pav}$), so that:

$$\overline{T}^{cool}_{pav} = \overline{T}_{pav} - \cos(\lambda_{sun}) \cdot \Delta T_{max} \quad (7)$$

where $\overline{T}^{cool}_{pav}$ is the surface temperature of cool pavement, λ_{sun} the zenith angle of the sun (in Deg), and ΔT_{max} the maximum temperature decrease it can be achieved by the cool pavement.

3. CASE STUDY

3.1 Studied area

The coupled scheme was trained and tested using data collected by Miguel et al. [16] during a field experiment between April and August 2019 in a university campus of Singapore. The field experiment was primarily aimed at measuring weather conditions at four vertical heights of a single position within a street canyon. The street canyon is surrounded by four buildings and is only paved with asphalt.

3.2 Weather conditions and surface temperature

Measurements taken by Miguel et al. [16] at 3, 6, 9, and 12 meters on a flux tower were used to evaluate $\overline{T}^m{}_{can}$ and $\overline{q}^m{}_{can}$ in the street canyon. In contrast with $\bar{T}^m{}_{can}$, $\bar{q}^m{}_{can}$ is not directly measured on the flux tower. It was assessed from the relative humidity measured at the four levels and the pressure at 3 meters. Both $\bar{T}^m{}_{can}$ and $\bar{q}^m{}_{can}$ were collected every 10 seconds. The mean over a 5-minute time frame was retained as measurement of $\bar{T}^m{}_{can}$ and $\bar{q}^m{}_{can}$. Measurements between June 6 and August 19 2019 were used to train and test the DDM. It means that the DDM was trained and tested on a dataset of 10368 samples of $\bar{T}^m{}_{can}$ and $\bar{q}^m{}_{can}$. The same amount of samples was used to specify $\bar{T}_{pav}$. $\bar{T}_{pav}$ was collected using a contact surface sensor.

3.3 Surrounding buildings

The street canyon where Miguel et al. [16] collected measurements of weather conditions is surrounded by four buildings: A, B, C, and D (see Figure 3). Their height varies from 15 to 24 meters, while the street canyon has a width of 10 meters.

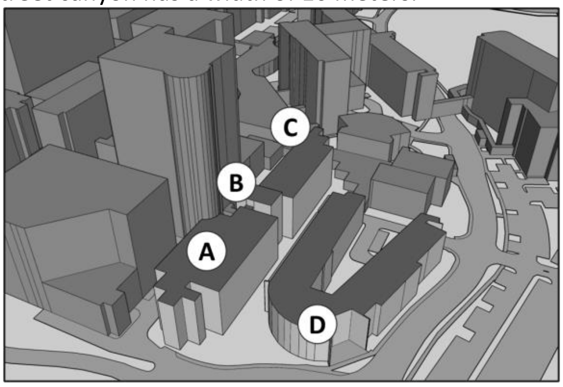

Figure 3. Buildings being modelled using EnergyPlus.

Buildings A, B, C, and D were modelled using EnergyPlus. Using this building energy simulation tool, it was possible to model buildings with LoD 1.2 as stated by Biljecki et al. [8]. Materials and internal heat gains were assigned from the Sketchup OpenStudio database (https://openstudio.net/) as those of typical office buildings in the tropics. An ideal load model was used to assess the amount of fresh air needed to keep the indoor temperature of buildings at 24 degrees Celsius and the relative humidity at 60%.

3.4 Baseline and scenarios

The baseline configuration refers to the original parameters of the coupled scheme that are used to evaluate increases or decreases in the outdoor air temperature or building energy demand caused by different scenarios. It was simulated using the Euler implicit method to discretize the linear state space model of the DDM. The multi-objective function stated in Equation (5) was optimized using the NSGA-2 method with h_{lb} equal to 0 Watts and h_{up} equal to 500 Watts. The convergence criteria was defined with $\varepsilon_{\bar{H}_{sys}}$ and $\varepsilon_{\overline{LE}_{sys}}$ equal to 0.01 Watts. The weather conditions at the atmospheric level were assumed to be equal to that recorded over a typical meteorological year in Singapore. In contrast with other scenarios, the baseline assumes that the outdoor conditions are not affected by waste heat releases and the surface temperature of the street is equal to measurements.

Therefore, scenarios aimed at estimating the impact of waste heat releases and cool pavement on the outdoor air temperature and building energy demand at the location where Miguel et al. [16] conducted their field experiment. Waste heat releases were assumed to be generated at a rate of 1.4 Watts per Watt of cooling consumed in buildings A, B, C, and D. It was also considered that 100% of them are sensible and go into the street canyon. In accordance with Anting et al. [17], it was supposed that cool pavement can achieve a decrease of 6.5 degrees Celsius at the highest exposure of the Sun.

4. RESULTS AND DISCUSSION

4.1 Simulations

In Figure 4, the hourly average outdoor air temperature as predicted by the DDM is shown in comparison to this assessed from measurements collected by Miguel et al. [16]. It is observed that the discrepancy between predictions and measurements is the lowest when the DDM is trained on 80% of measurements. It is usually expected that the accuracy of a DDM increases with respect to the size of its training set. Despite this observation, it is seen that the discrepancy between predictions and observations is higher at daytime than nighttime, that is when variations of the outdoor air temperature are the highest. This result certainly originates from the fact that $\boldsymbol{h}$ is assumed to be constant over time. From a physical point of view, its value is affected by wind speed and direction in the street canyon, and therefore, should vary over the day.

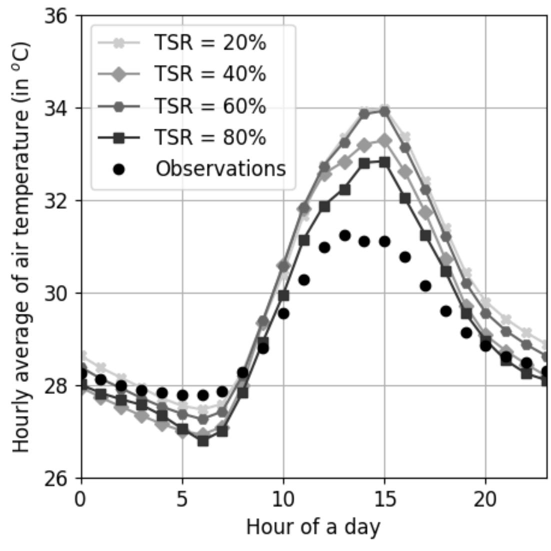

Figure 4. Average daily cycle of outdoor air temperature as measured by weather stations (dot) and as predicted by the DDM using different Training Split Ratios (TSR).

Although a time-constant $\boldsymbol{h}$ seems to limit the accuracy that can be achieved by the coupled scheme at daytime, results illustrated Table 1 show that the RMSE and MBE of the outdoor air temperature falls below 2.5 and 1.0 degrees Celsius, respectively, whichever split ratio is used to train the DDM. According to Miguel et al. [16], it is an acceptable accuracy when typical meteorological data are used to specify weather conditions at the atmospheric level. The accuracy of the coupled scheme could thus be improved if weather conditions at the atmospheric level were defined from measurements at the rooftop level or from simulations of a climate model.

Table 1. Root Mean Square Error (RMSE) and Mean Bias Error (MBE) between predictions and measurements of the outdoor air temperature and humidity using different Training Split Ratios (TSR).

TSR	Temperature		Humidity		Size test samples
	RMSE (K)	MBE (K)	RMSE (g/kg)	MAE (g/kg)	
20%	2.24	0.93	6.80	5.90	8291
40%	2.24	0.39	4.19	3.67	6219
60%	2.31	0.80	5.46	4.76	4146
80%	2.16	0.23	4.42	3.82	2074

4.2 Baseline-scenario analysis

From results shown in Figure 5, it seems that the outdoor air temperature would not be highly affected if waste heat was released in the street canyon connecting buildings A, B, C, and D. This result can be justified by the fact that buildings A, B, C, and D have a relatively small volume in comparison to other buildings that can be observed in the central business district of Singapore. However, it is important to note that the building consumption, as well as the waste heat releases, are certainly underestimated by the DDM in the case of Singapore. The main reason is that the 3D city model used to develop detailed BEMs was of a LoD 1.2, and thus, had no information about dimensions and positions of windows. As a consequence, buildings were assumed to be fully covered by walls, which neglects the impact of solar heat penetration on their cooling consumption.

Figure 6 illustrates the effect of cool pavement in the outdoor air temperature as predicted by the DDM. As expected, the highest decrease in the outdoor air temperature appears to be achieved between noon and 4pm. Although the effect of cool pavement on the outdoor air temperature can clearly be observed from predictions of the DDM, it should not be the only countermeasure to be considered by the coupled scheme. In addition to cool pavement, the coupled scheme should also be able to evaluate the impact of vegetation, another countermeasure to UHIs.

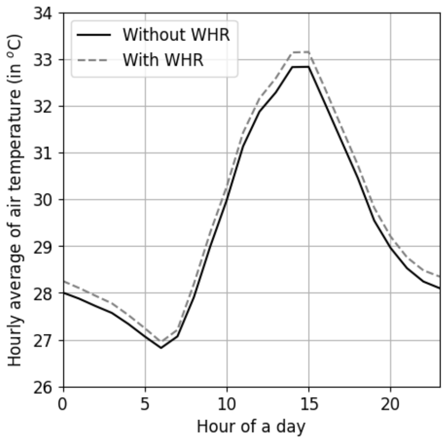

Figure 5. Average daily cycle of the outdoor air temperature predicted by the DDM with and without considering Waste Heat Releases (WHR) of buildings A, B, C, and D.

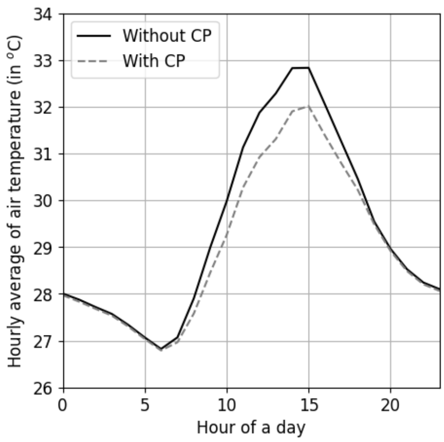

Figure 6. Average daily cycle of the outdoor air temperature predicted by the DDM with and without considering Cool Pavement (CP) in the street canyon.

Table 2 shows the average and highest impact of waste heat releases and cool pavement on the outdoor air temperature in the street canyon and the total sensible cooling load of buildings A, B, C, and D as assessed from the baseline. While waste heat releases appear to increase both the outdoor air temperature and the sensible cooling load, their magnitude looks to be reduced by cool pavement. Even though the result is consistent with expectation on the impact of waste heat releases and cool pavement, their accuracy could have been improved if detailed BEMs had been calibrated against measurements of the cooling load. Unfortunately, no metered data was collected during the experiment conducted by Miguel et al. [16].

Table 2. Average difference (Avg. diff.) and peak difference (Peak diff.) between the baseline and scenarios comprising Waste Heat Releases (WHR) and Cool Pavement (CP).

Scenario	Air Temperature		Sensible cooling load	
	Avg. diff. (K)	Peak diff. (K)	Avg. diff. (kW)	Peak diff. (kW)
WHR	0.25	0.67	1.78	4.69
CP	-0.34	-1.15	-3.90	-16.67

5. CONCLUSION

This study explained how interactions between buildings and their outdoor conditions can be simulated using a coupling between detailed BEMs and a data driven UCM. The DDM was trained and tested using measurements of outdoor air temperature and humidity collected in Singapore by Miguel et al. [16]. The DDM was also used to observe the impact of waste heat releases and cool pavement on the outdoor air temperature of the street canyon and the cooling consumption of buildings.

One result was that the DDM predicts the outdoor air temperature with a similar accuracy than the physically-based model validated by Miguel et al. [16] using the same input and test data. At the same time, it was shown that the DDM predicts the outdoor air temperature with a higher temporal resolution than the physically-based model while considering urban morphology with a higher level of detail. It means a DDM is certainly a more appropriate solution to predict outdoor conditions at the neighbourhood scale within a CDT than any physically-based UMM that can be coupled with detailed BEMs.

Another result was that the DDM is capable of predicting the impact of waste heat releases and cool pavement on outdoor conditions of a street canyon, which is a major improvement in comparison to other DDMs described in the literature [4]. This improvement was possible by defining a DDM that is still governed by fundamental principles of heat and mass transfer. Using the same principles, the DDM could easily consider additional sources of anthropogenic heat like traffic or countermeasures to UHIs like vegetation.

ACKNOWLEDGEMENTS

This research has received funding from the European Union's Horizon research and innovation programme under the Marie Sklodowska-Curie grant agreement No 101059484. The data were collected during the Virtual Campus project at the National University of Singapore, which was sponsored by the University Campus Infrastructure and the Office of the Deputy President.

REFERENCES

1. Srivastava, K. (2009). Urbanization and mental health. *Industrial psychiatry journal*, 18(2): p. 75.
2. Niranjan, A. *'Era of global boiling has arrived,' says UN chief as July set to be hottest month on record*. [Online] Available from: https://www.theguardian.com/science/2023/jul/27/scientists-july-world-hottest-month-record-climate-temperatures [27 July 2023].
3. Jamei, E., et al. (2016). Review on the impact of urban geometry and pedestrian level greening on outdoor thermal comfort. *Renewable and Sustainable Energy Reviews*, 54: p. 1002-1017.
4. Quan, S.J. and C. Li. (2021). Urban form and building energy use: A systematic review of measures, mechanisms, and methodologies. *Renewable and Sustainable Energy Reviews*, 139: p. 110662.
5. Schrotter, G. and C. Hürzeler. (2020). The Digital Twin of the City of Zurich for Urban Planning. *PFG – Journal of Photogrammetry, Remote Sensing and Geoinformation Science*, 88(1): p. 99-112.
6. Deng, T., K. Zhang, and Z.-J. Shen. (2021). A systematic review of a digital twin city: A new pattern of urban governance toward smart cities. *Journal of Management Science and Engineering*, 6(2): p. 125-134.
7. Li, X., et al. (2022). Big data analysis of the Internet of Things in the digital twins of smart city based on deep learning. *Future Generation Computer Systems*, 128: p. 167-177.
8. Biljecki, F., H. Ledoux, and J. Stoter. (2016). An improved LOD specification for 3D building models. *Computers, Environment and Urban Systems*, 59: p. 25-37.
9. Deilami, K., M. Kamruzzaman, and Y. Liu. (2018). Urban heat island effect: A systematic review of spatio-temporal factors, data, methods, and mitigation measures. *International Journal of Applied Earth Observation and Geoinformation*, 67: p. 30-42.
10. Li, X., et al. (2019). Urban heat island impacts on building energy consumption: A review of approaches and findings. *Energy*, 174: p. 407-419.
11. Sezer, N., et al. (2023). Urban microclimate and building energy models: A review of the latest progress in coupling strategies. *Renewable and Sustainable Energy Reviews*, 184: p. 113577.
12. Jandaghian, Z. and U. Berardi. (2020). Comparing urban canopy models for microclimate simulations in Weather Research and Forecasting Models. *Sustainable Cities and Society*, 55: p. 102025.
13. Toparlar, Y., et al. (2017). A review on the CFD analysis of urban microclimate. *Renewable and Sustainable Energy Reviews*, 80: p. 1613-1640.
14. Wang, H., et al. (2023). Machine learning applications on air temperature prediction in the urban canopy layer: A critical review of 2011–2022. *Urban Climate*, 49: p. 101499.
15. Grimmond, C.S.B. (2006). The suburban energy balance: Methodological considerations and results for a mid-latitude west coast city under winter and spring conditions. *International Journal of Climatology*, 12(5): p. 481-497.
16. Miguel, M., et al. (2021). A physically-based model of interactions between a building and its outdoor conditions at the urban microscale. *Energy and Buildings*, 237: p. 110788.
17. Anting, N., et al. (2017). Experimental evaluation of thermal performance of cool pavement material using waste tiles in tropical climate. *Energy and Buildings*, 142: p. 211-219.

WUST Publishing House prints can be obtained
via mailorder: zamawianie.ksiazek@pwr.edu.pl;
www.ksiegarnia.pwr.edu.pl

ISBN 978-83-7493-275-2